

Ab initio studies of silane decomposition on Si(100)

Ze Jing

Department of Physics, North Carolina State University, Raleigh, North Carolina 27695-8201

Jerry L. Whitten

Department of Chemistry, North Carolina State University, Raleigh, North Carolina 27695-8201

(Received 28 January 1991)

The mechanism of silane decomposition on the Si(100)-(2×1) surface is investigated in the context of a many-electron theory that permits the accurate computation of molecule-solid surface interactions at an *ab initio* configuration-interaction level. The adsorbate and local surface region are treated as embedded in the remainder of the lattice electronic distribution, which is modeled as a three-layer, 19-Si-plus-21-H cluster. A possible energetic pathway is found for the reaction $\text{SiH}_4 \rightarrow \text{SiH}_3 + \text{H}$ on the surface. It involves two separate steps: (1) scission of one Si—H bond; (2) formation of two bonds to SiH_3 and H from two surface dangling bonds. The energy barrier, which is calculated to be 9 kcal/mol, occurs in the first step at a distance of 3.6 Å from the Si in SiH_4 to a Si surface atom with a Si—H bond aligned with a surface dangling-bond direction. The overall dissociation process $\text{SiH}_4 \rightarrow \text{SiH}_3 + \text{H}$ on the surface is found to be 2.8 eV exothermic. Quantum tunneling is found to play an important role in the process at room temperature. A symmetrical Eckart potential is used to estimate the quantum tunneling effect and the reaction probability is calculated to be small (on the order of 10^{-5}) and relatively insensitive to the silane temperature.

I. INTRODUCTION

Although there have been numerous experimental studies,^{1–18} the details of Si chemical vapor deposition (CVD) from silane are not well understood. The processes are very complex and may involve several steps:¹⁷ (1) SiH_4 adsorption; (2) Si—Si bond formation; (3) decomposition and diffusion of SiH_x species; and (4) $\text{H}_2(g)$ evolution. Most of the experimental work^{1–16,18} has dealt with the overall reaction $\text{SiH}_4(g) \rightarrow \text{Si}(s) + \text{H}_2(g)$, and only indirect information is obtained on the mechanism of silane decomposition. Hirva and Pakkanen,¹⁹ in theoretical work, obtained qualitative estimates of energies for possible reaction mechanisms of SiH_4 .

Buss and co-workers¹⁸ have studied SiH_4 adsorption and Si growth on polycrystalline Si for a wide range of temperature and flux conditions and have found that the reactive sticking coefficients (RSC) have non-Arrhenius temperature dependences and decrease with increasing flux at low temperature. They attributed the small RSC (less than 0.004) to the existence of a potential-energy barrier in the adsorption of silane on the surface, which could be surmounted by translational or vibrational energy of the silane molecules rather than thermal energy from the surface. They calculated that a silane adsorption barrier of 4 kcal/mol would account for the low RSC, i.e., only 0.004 of room-temperature silane molecules have the internal or translational energy above 4 kcal/mol. If this explanation for the low RSC of silane is valid, then heating the silane should dramatically increase the reaction rate. However, they found that the effect of heating (unspecified magnitude) is not significant.

Recently, Gates *et al.*¹⁷ studied the mechanism of

silane decomposition directly on Si(111)-(7×7) and Si(100)-(2×1) surfaces below 500°C, under ultrahigh vacuum (UHV) conditions, using static secondary-ion mass spectrometry (SSIMS) to identify the surface SiH_x species. Based on the finding that the adsorption of silane on the Si(100)-(2×1) surface produces only SiH_3 and H at low temperature, they proposed a model that involves scission of one Si—H bond in SiH_4 and formation of two new bonds to the H and SiH_3 fragments from two dangling bonds on two adjacent surface Si atoms. The two dangling bonds could be on dimerized atoms, or on two atoms from two adjacent dimers. Concerning the very small RSC by a silane molecule (10^{-5} on defects, and less on the average surface), they suggested that the molecular internal energy is more important than surface structure effects in controlling the adsorption rate and that a barrier of 3.3 kcal/mol exists in the adsorption of silane on single-crystal Si.

The objective of the present work is to look for a possible energetic pathway for the model proposed by Gates *et al.* and to understand the mechanism of silane decomposition on the Si(100)-(2×1) surface. The quantum-mechanical study is conducted in the context of a many-electron theory that permits the accurate computation of molecule-solid surface interactions at an *ab initio* configuration-interaction level. The adsorbate and local surface region are treated as embedded in the remainder of the lattice electronic distribution, which is modeled as a three-layer, 19-Si-plus-21-H cluster. Section II gives a brief review of the general theory. Section III reports the results of some related small molecule studies. The results of the silane decomposition calculations and discussion are presented in Sec. IV and the conclusions are summarized in Sec. V.

II. THEORY AND COMPUTATIONAL METHODS

The objective of the theory is to treat the surface region and adsorbed species with sufficient accuracy to describe reaction energetics, while at the same time maintaining a proper coupling of the surface region to the bulk.²⁰⁻²² Calculations are performed by first obtaining self-consistent-field (SCF) solutions for the cluster. The occupied and virtual orbitals of the SCF solution are then transformed separately to obtain orbitals spatially localized about the surface atoms. This unitary transformation of orbitals is based on exchange maximization with the valence orbitals of atoms belonging to the adsorbate and local region and is designed to enhance convergence of the configuration-interaction (CI) expansion. The CI calculation involves excitation within a 27-electron subspace to 24 possible virtual localized orbitals. All configurations arising from single and double excitations with an interaction energy greater than 5×10^{-6} hartrees with the parent SCF configuration are explicitly retained in the expansion; contributions of excluded configurations are estimated using second-order perturbation theory. All the configurations with relative large coefficients (>0.06) are taken as parent configurations, and the CI procedure described above is repeated.

Two silicon basis sets are employed in the calculations: one is the double-zeta five-term $3s$ and four-term $3p$ set used in Ref. 23 augmented by a set of d functions, and the other is a five-term T (tetrahedral) basis set.²⁴ By placing functions f_i ($i=1,2,3,4$) along the four tetrahedral directions, where f_i consist of N -term primitive Gaussians, it has been proved that the four tetrahedral functions can be used to represent both the $3s$ and $3p$ orbitals. The coefficients in the s and p expansions are derived from a common function by varying the displacements and the only constraint is that their exponents be the same. With the same number of basis functions, calculations with the T basis are significantly faster than with the sp basis. Due to the large displacements, the T basis is not rotationally invariant, but this shortcoming is eliminated by placing the lobes in the Si bond directions. The T basis is used for atoms outside the local region of the cluster. Atoms in the local region are described by the double-zeta s and p basis, augmented by a single set of d functions (with exponent 0.4). The H atoms in the SiH_4 molecule are described by a double-zeta basis s, s' and a single Gaussian p function with an exponent of 0.6. A four-term basis is used for H atoms that are used to saturate the peripheral silicon atoms of the cluster.

III. BASIS TEST AND SILANE DECOMPOSITION SIMULATION

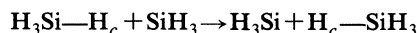
In this section, we will consider the reaction of $\text{SiH}_4 + \text{SiH}_3 \rightarrow \text{SiH}_3 + \text{SiH}_4$ to simulate the process of H transferring from SiH_4 to a silicon surface.

Both SiH_3 and SiH_4 are well-studied molecules.²⁵⁻²⁸ The SiH_3 radical has a pyramidal structure, a roughly tetrahedral bond angle, and a Si—H bond length of 1.47 Å. A similar structure and Si—H bond length are cited for the SiH_4 molecule. Our calculations show that both

SiH_3 and SiH_4 have a tetrahedral structure and the Si—H bond length is found to be 1.50 Å. In a further test of our basis set and Si pseudopotential, we compare our calculated geometries and H dissociation energy of SiH_4 with the results from all-electron calculations using Dunning's $6s/4p$ basis.²⁹ The geometries are found to be nearly identical and the H binding energy at the SCF level differs by only 0.03 eV.

One important feature we note from the SiH_4 molecular study is that removing a H or replacing a H with a SiH_3 radical in a SiH_4 molecule does not appreciably affect the bond length or geometry of the remaining H atoms. Thus, during the scission of one Si—H bond in SiH_4 , the remaining three Si—H bonds will be fixed at the tetrahedral bond angle with a bond length of 1.50 Å.

Previous calculations³⁰ have shown that chemisorbed H on the Si(100) surface has a binding energy of 3.7 eV, similar to the 3.9-eV SiH bond energy in a SiH_4 molecule. Therefore, it seems reasonable to use a SiH_3 radical to simulate a surface site in the preliminary study. The process considered is a simple H transfer between SiH_4 and SiH_3 , written as



as depicted in Fig. 1. Since a Si—H bond must be partially broken in order to transfer the H, an energy barrier likely exists. We consider the activated complex $\text{H}_3\text{Si—H}_c\text{—SiH}_3$, with reaction coordinate Si—H_c—Si and the saddle point at the center. Minimization of the energy at the saddle point with respect to the distance $R_{\text{Si-Si}}$ gives an energy barrier of 9 kcal/mol at $R_{\text{Si-Si}} = 3.6$ Å. Table I lists the points calculated, where the optimizations are also performed for the Si—H bond length and angle. As expected, the Si—H bond lengths and angle are nearly identical to that in SiH_3 . From the very small energy difference between the eclipsed and staggered form of the Si_2H_6 molecule (with a rotation barrier of only 0.55 kcal/mol),³¹ we conclude that the activated complex can rotate essentially freely; therefore, no optimization is done on the relative orientation of the two SiH_3 species. The basis set and pseudopotential method are also tested for this reaction for a number of geometries. Compared

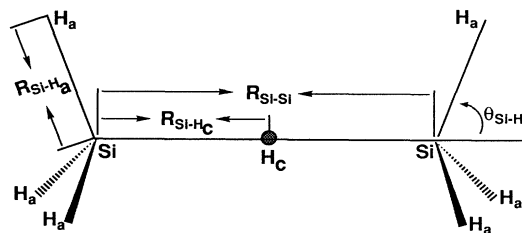


FIG. 1. The process of hydrogen transfer between SiH_4 and SiH_3 . $R_{\text{Si-H}_c}$ is the distance between the transfer hydrogen, H_c , and the nearest Si atom. $R_{\text{Si-H}_a}$ is the distance between the terminal hydrogens, H_a , and the nearest Si atom and $\theta_{\text{Si-H}}$ is the angle between Si—H_a and the Si—Si bond axis.

TABLE I. SCF and CI energies of Si_2H_7 as functions of $R_{\text{Si-Si}}$, $R_{\text{Si-H}_c}$, $R_{\text{Si-H}_a}$, and $\theta_{\text{Si-H}}$ (shown in Fig. 1). Energies and distances are in a.u. (One a.u. of length equals 0.529 18 Å and one a.u. of energy equals 27.211 eV or 627.51 kcal/mol).

$R_{\text{Si-Si}}$	$R_{\text{Si-H}_c}$ ^a	$R_{\text{Si-H}_a}$ ^b	$\theta_{\text{Si-H}_a}$ ^c	E_{SCF}	E_{CI}
6.6	3.3	2.9	54.7	-11.365 03	-11.514 90
6.8	3.4	2.9	54.7	-11.365 48	-11.516 53
7.0	3.5	2.9	54.7	-11.364 18	-11.515 31
6.8	3.4	2.7	54.7	-11.360 26	-11.508 28
6.8	3.4	2.8	54.7	-11.366 09	-11.517 87
6.8	3.4	2.9	54.7	-11.365 48	-11.516 53
6.8	3.4	3.0	54.7	-11.359 71	-11.514 24
6.8	3.4	2.9	49.7	-11.362 86	-11.515 11
6.8	3.4	2.9	54.7	-11.365 48	-11.516 53
6.8	3.4	2.9	59.7	-11.362 96	-11.516 15
6.6	2.9	2.9	54.7	-11.371 58	-11.520 70
6.8	2.9	2.9	54.7	-11.376 84	-11.524 95
7.0	2.9	2.9	54.7	-11.381 36	-11.528 23
7.4	2.9	2.9	54.7	-11.388 55	-11.533 01
20.0	2.9	2.9	54.7	-11.400 83	-11.531 14

^aThe distance between the transfer hydrogen, H_c , and the nearest Si atom.

^bThe distance between the terminal hydrogens, H_a , and the nearest Si atom.

^cThe angle between Si-H_a and the Si—Si bond axis.

with the all-electron results using Dunning's basis, the difference in the relative energy is found to be within 0.05 eV.

IV. SILANE DECOMPOSITION

The cluster used to simulate the Si(100)-(2×1) surface has been developed in previous work.³⁰ It consists of nine Si atoms in the surface layer, six in the second layer, and four in the third layer as shown in Fig. 2. All of the peripheral dangling bonds of the boundary atoms are saturated by H atoms along the bond direction with a Si—H bond length of 1.5 Å. Previous calculations³² have found that the electronic properties of the cluster are not sensitive to the distance between the boundary silicon atoms and their hydrogen saturators. The three additional H atoms on the surface plane have slightly different roles. Besides saturating the surface dangling bonds, they are used to balance the force on the three surface Si atoms; these H saturators will move in the x direction (the direction of Si-Si pairing) accordingly during the surface reconstruction. The nearest Si-Si distance is taken to be the bulk bond length of 2.35 Å for all the Si atoms in the cluster. Calculations on this cluster have shown that the surface atoms will reconstruct to form dimers, and the dimer bond length was found to be 2.48 Å,³⁰ which is consistent with other theoretical and experimental work. The study of H chemisorption on the surface shows that the adsorption of a single H atom, or H atoms in the monohydride phase, does not change the surface reconstruction. Thus, we would not expect interaction of H with the surface in the silane dissociation process to

change the surface reconstruction appreciably.

There are three characteristic lengths on the Si(100)-(2×1) surface: $R_{2,3}=5.18$ Å, $R_{2,5}=3.81$ Å, and $R_{1,2}=2.43$ Å, where 1, 2, and 5 are the atoms numbered in Fig. 2. The size (H-H distance) of a SiH_4 molecule is about 2.49 Å. Based on size, if the dissociation process takes place by the interaction of SiH_4 with two surface sites, it would most likely occur above the middle point of a Si-Si dimer. The Si—H bond direction in the SiH_4 molecule, however, does not match the surface-dangling-bond direction, and further, bond formation would require breaking the dimer. The calculated energy for this site turns out to be very high, and thus the two-site dissociation process appears unfavorable.

For the one-site dissociation process, the process is similar to the $\text{SiH}_3 + \text{SiH}_4$ study in Sec. III: the activated complex is taken as $\text{H}_3\text{Si-H}_c\text{-Si(100)}$ with reaction coordinate Si— H_c —Si. However, there are several possible differences: (1) the saddle point may not be in the center since the activated complex is no longer symmetrical; (2) the reaction coordinate Si— H_c —Si may not be linear because of the effect of the surface; and (3) the Si— H_c bond direction is determined by the surface-dangling-bond direction. In the total-energy calculations, we define $R_{\text{Si-Si}}$, $R_{\text{Si-H}}$, θ_x , θ_y , and φ_x , as depicted in Fig. 3. The calculated energies are reported in Tables II and III. The saddle point is found at $R_{\text{Si-H}_c}=1.8$ Å and $R_{\text{Si-Si}}=3.6$ Å, the same as in the $\text{H}_3\text{Si-H-SiH}_3$ transition state. Table II shows that the energy decreases when the central H moves away from the saddle point. Using the harmonic approximation, the imaginary frequency is cal-

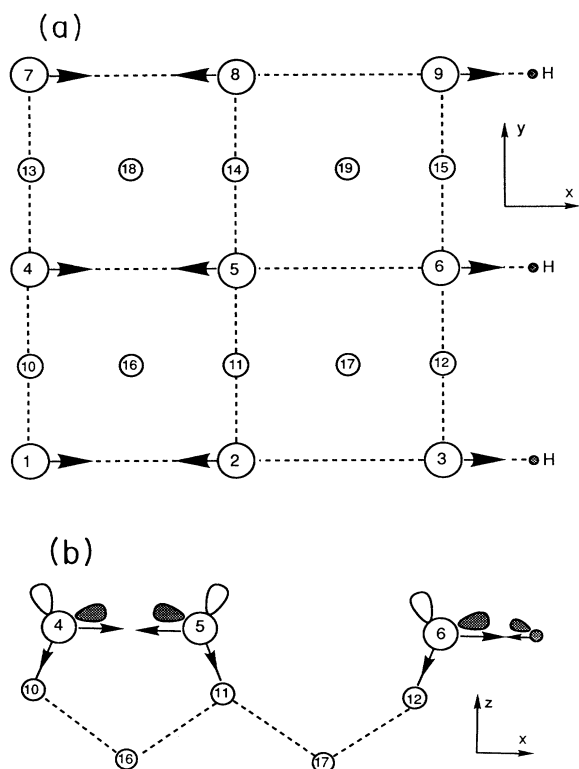


FIG. 2. Top view showing the displacement of atoms in the reconstruction of the Si(100) surface and side view of the reconstructed surface; Si_{19} cluster model of Si(100). Three H atoms are bonded to surface Si atom 3, 6, and 9, respectively, to balance the force on these atoms by simulating the missing surface atoms. There are 21 additional H saturators that are not shown here. The open orbitals represent surface dangling bonds and the shaded orbitals represent contributions to the dimer bond.

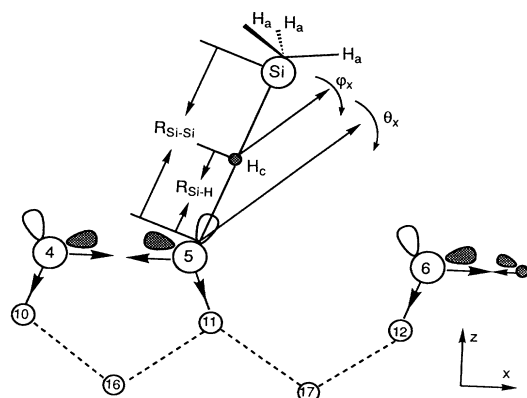


FIG. 3. Silane dissociation process. $R_{\text{Si-Si}}$ is the distance between the Si in the SiH_4 molecule and the surface Si atom (numbered 5) and $R_{\text{Si-H}}$ is the distance between the transfer hydrogen, H_c , and the surface Si atom. θ_x and θ_y (not shown in the graph) are the angles of rotation of $\text{H}_c\text{-Si-H}_3$ from the direction of the surface dangling bond about surface atom 5 clockwise and into the page, respectively. φ_x is the angle of rotation of SiH_3 from the surface-dangling-bond direction around the H_c atom.

TABLE II. SCF and CI energies of $\text{SiH}_4/\text{Si}_{19}$ as functions of $R_{\text{Si-Si}}$ and $R_{\text{Si-H}}$ (shown in Fig. 3). Energies and distances are in a.u.

$R_{\text{Si-Si}}^a$	$R_{\text{Si-H}}^b$	E_{SCF}	E_{CI}
6.8	2.9	-87.264 39	-87.400 07
6.8	3.2	-87.257 59	-87.397 46
6.8	3.4	-87.256 26	-87.395 51
6.8	3.6	-87.260 01	-87.398 56
6.6	3.3	-87.256 52	-87.395 49
6.8	3.4	-87.256 26	-87.395 51
7.0	3.5	-87.254 11	-87.393 31
20.0	17.1	-87.289 27	-87.415 77

^aThe distance between the Si in the SiH_4 molecule and the surface Si atom.

^bThe distance between the transfer hydrogen, H_c , and the surface Si atom.

culated to be 1817 cm^{-1} . All variations of bond angles relative to both x and y axes from the surface-dangling-bond direction result in higher energies. We conclude that the electronic energy barrier, which is calculated to be 12.6 kcal/mol , occurs at the middle of Si—Si bond along the surface-dangling-bond direction with $R_{\text{Si-Si}} = 3.6 \text{ \AA}$.

Once the H transfers from SiH_4 and forms a bond with the surface atom, the resulting SiH_3 radical will experience a repulsive force and will migrate to another surface site. Table IV shows that the energy of the system decreases when the SiH_3 radical moves away from the surface site in the x , y , or z directions. Since SiH_3 has a singly occupied dangling bond, it can easily bind to another surface dangling bond. Table V reports the results for reaction at the site shown in Fig. 4. These calculations are carried out with the Si— H_c bond length fixed at 1.53 \AA . The energy minimum occurs at $R_{\text{Si-Si}} = 2.37 \text{ \AA}$. The overall dissociation process $\text{SiH}_4 \rightarrow \text{SiH}_3 + \text{H}$ on the surface is found to be 2.8 eV exothermic.

TABLE III. SCF and CI energies of $\text{SiH}_4/\text{Si}_{19}$ as functions of θ_x , φ_x , and θ_y (shown in Fig. 3). Energies are in a.u.

θ_x	φ_x	θ_y	E_{SCF}	E_{CI}
5°	0°	0°	-87.255 85	-87.395 22
0°	0°	0°	-87.256 26	-87.395 51
-5°	0°	0°	-87.255 33	-87.394 44
0°	5°	0°	-87.254 92	-87.394 19
0°	0°	0°	-87.256 26	-87.395 51
0°	-5°	0°	-87.252 82	-87.392 00
0°	0°	20°	-87.254 76	-87.389 84
0°	0°	10°	-87.257 67	-87.392 79
0°	0°	0°	-87.256 26	-87.395 51

TABLE IV. SCF and CI energies of $\text{SiH}_3 + \text{H}/\text{Si}_{19}$ as functions of SiH_3 displacement Δd in the x , y , and z directions, respectively, while the center H_c atom binds to surface atom 5 with a bond length of 2.9 a.u. The first row is from the starting geometry, i.e., $R_{\text{Si-Si}} = 6.8$ a.u. and $R_{\text{Si-H}} = 2.9$ a.u. (see Fig. 3). Energies and distances are in a.u.

Axis	Δd	E_{SCF}	E_{CI}
	0.0	-87.264 39	-87.400 07
x	0.2	-87.264 51	-87.400 82
y	0.2	-87.266 02	-87.402 00
z	0.2	-87.267 61	-87.403 06

In the comparison of our calculated electronic energy barrier with the experimental measured value of 4 kcal/mol, several factors should be considered: (1) zero point vibrational energy; (2) thermal translational and vibrational energy; and (3) quantum tunneling. Incorporation of the zero-point vibrational energy reduces the barrier to 9 kcal/mol. At temperature T , the probability of finding silane molecules³³ that have internal or vibrational energy between E and $E + \Delta E$ can be expressed as $P_E = \exp(-E/kT)\Delta E/kT$. The transmission coefficient³³ from quantum tunneling using the symmetrical Eckart potential can be expressed as follows:

$$T_E = [\cosh(2an^{1/2}) - 1] / [\cosh(2an^{1/2}) + \cosh(4a^2 - \pi^2)]^{1/2},$$

where $n = E/V$, $a = 2\pi V/hf$, V is the barrier height, and f is the imaginary frequency at the saddle point. Thus, the probability of H transfer at temperature T is the integration of T_E over the Boltzmann distribution P_E . The results, $\log_{10}(P)$ vs $1/T$, are plotted in Fig. 5. Several features are immediately clear. First, the curve is not linear and relatively flat, suggesting that quantum tunneling plays an important role, especially at low temperature. This would help explain the experimental observation that the effect of temperature does not change the reaction rate dramatically. Second, the reaction probability is very small, possibly on the order of 10^{-5} , which is within the range of the experimentally measured RSC of less than 10^{-5} . On the other hand, the one-dimensional Eckart potential has been known to overestimate the tunneling effect, and thus these results are at best qualitative. We would not speculate on the detailed comparison with the experimental RSC, which has a large error and is further complicated by other factors,

TABLE V. SCF and CI energies of $\text{SiH}_3 + \text{H}/\text{Si}_{19}$ as a function of $R_{\text{Si-Si}}$. H_c has a SiH bond length of 2.9 a.u. (see Fig. 4). Energies and distances are in a.u.

$R_{\text{Si-Si}}$	E_{SCF}	E_{CI}
4.2	-87.380 86	-87.511 26
4.4	-87.386 96	-87.517 69
4.6	-87.386 71	-87.517 11

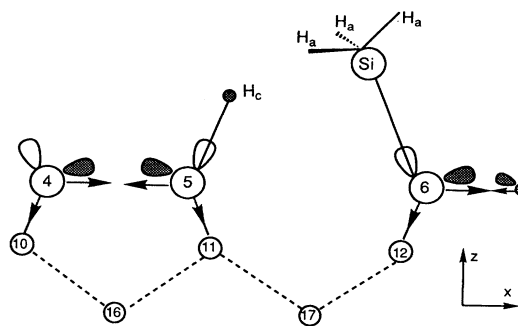


FIG. 4. After silane dissociation, the H_c binds to a surface site and the SiH_3 radical binds to another site. $R_{\text{Si-Si}}$ is the distance between the Si in the SiH_3 radical and the surface Si atom (numbered 6).

especially the surface coverage. Also, the graph shows that the reaction probability is very sensitive to the barrier height. A 10% change in the barrier height results in a nearly threefold change in the reaction probability. It is not clear how accurate our calculated activation barrier is, however, and errors of several kcal/mol are certainly possible. Furthermore, it is possible that there exist energetic pathways that have a similar or lower-energy barrier. To enable reasonable molecular-dynamics calculations, much more extensive work would be needed to generate a more extensive energy surface. Only then can we accurately predict the temperature dependence of the dissociation rate.

V. SUMMARY

(1) The mechanism of silane decomposition on the $\text{Si}(100)-(2 \times 1)$ surface is investigated in the context of a

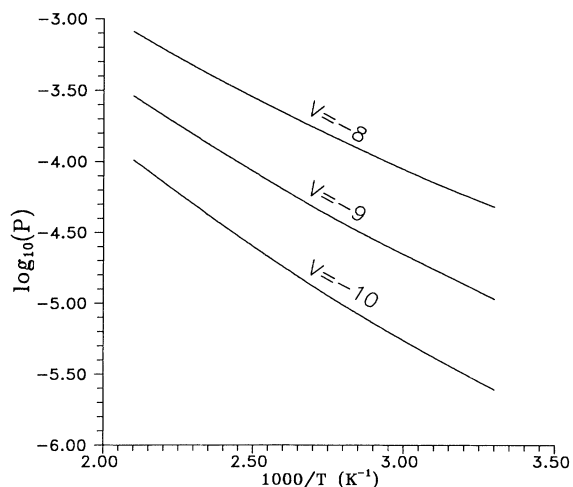


FIG. 5. The plot of $\log_{10}(P)$ vs $1/T$, where P is the sticking coefficient and T is the temperature.

many-electron theory that permits the accurate computation of molecule-solid surface interactions at an *ab initio* configuration-interaction level. The adsorbate and local surface region are treated as embedded in the remainder of the lattice electronic distribution, which is modeled as a three-layer, 19-Si-plus-21-H cluster.

(2) The reaction $\text{SiH}_4 \rightarrow \text{SiH}_3 + \text{H}$ on the surface may involve two separate steps: (i) scission of one Si—H bond; (ii) formation of two new bonds to SiH_3 and H from two surface dangling bonds. The energy barrier, which is calculated to be 9 kcal/mol (including the zero vibrational energy correction), occurs in the first step with a Si—H bond aligned with the surface dangling bond at $R_{\text{Si-Si}} = 3.6 \text{ \AA}$. The overall dissociation process $\text{SiH}_4 \rightarrow \text{SiH}_3 + \text{H}$ on the surface is found to be 2.8 eV exothermic.

(3) Quantum tunneling is found to play an important role, and may dominate the dissociation process at room temperature. A symmetrical Eckart potential is used to estimate the quantum tunneling effect and the reaction probability is calculated to be small (possibly on the order of 10^{-5}) and relatively insensitive to the silane temperature.

ACKNOWLEDGMENTS

This research was supported by a grant from the U.S. Department of Energy and a grant of computer time from the North Carolina Supercomputer Center. One of the authors (Z.J.) would like to thank Dr. H. H. Carmichael for the helpful discussion of molecular kinetic theory.

-
- ¹R. F. C. Farrow, *J. Electrochem. Soc.* **121**, 899 (1974).
²J. Comfort and R. Reif, *J. Electrochem. Soc.* **136**, 2386 (1989).
³B. A. Joyce and R. R. Bradley, *Philos. Mag.* **14**, 289 (1966).
⁴B. A. Joyce, R. R. Bradley, and G. R. Booke, *Philos. Mag.* **15**, 1167 (1967).
⁵B. A. Joyce, R. R. Bradley, and B. E. Watts, *Philos. Mag.* **19**, 403 (1968).
⁶R. Robertson and A. Gallagher, *J. Chem. Phys.* **85**, 3623 (1986).
⁷D. J. Robbins and I. M. Young, *Appl. Phys. Lett.* **50**, 1575 (1987).
⁸W. A. P. Claassen, J. Bloem, W. G. J. N. Valkenburg, and C. H. J. Van den Brekel, *J. Cryst. Growth* **57**, 259 (1982).
⁹B. S. Meyerson and J. M. Jasinski, *J. Appl. Phys.* **61**, 785 (1987).
¹⁰D. W. Foster, A. J. Learn, and T. I. Kamins, *J. Vac. Sci. Technol. B* **4**, 1182 (1986).
¹¹R. S. Rosler, *Solid State Technol.* April, 63 (1977).
¹²T. J. Donahue and R. Reif, *J. Electrochem. Soc.* **133**, 1691 (1986).
¹³M. L. Hitchman, J. Kane, and A. E. Widmer, *Thin Solid Films* **59**, 231 (1979).
¹⁴C. H. J. van den Brekel and L. J. M. Bollen, *J. Cryst. Growth* **54**, 310 (1981).
¹⁵S. Gates, *Surf. Sci.* **195**, 307 (1988).
¹⁶S. M. Gates, C. M. Greenlief, D. B. Beach, and R. R. Kunz, *Chem. Phys. Lett.* **92**, 3144 (1990).
¹⁷S. M. Gates, C. M. Greenlief, D. B. Beach, and P. A. Holbert, *J. Chem. Phys.* **92**, 7493 (1990).
¹⁸R. J. Buss, P. Ho, W. G. Breiland, and M. E. Coltrin, *J. Appl. Phys.* **63**, 2808 (1988).
¹⁹P. Hirva and T. A. Pakkanen, *Surf. Sci.* **220**, 137 (1989).
²⁰C. Malvido and J. L. Whitten, *Phys. Rev. B* **26**, 4458 (1982).
²¹J. L. Whitten, *Phys. Rev. B* **24**, 1810 (1981).
²²P. Cremashi and J. L. Whitten, *Surf. Sci.* **149**, 273 (1985).
²³A. Chattopadhyay, P. V. Madhavan, J. L. Whitten, C. R. Fischer, and I. P. Batra, *J. Mol. Struct. (Theochem)* **163**, 63 (1988).
²⁴Ze Jing and J. L. Whitten (unpublished).
²⁵D. S. Marynick, *J. Chem. Phys.* **74**, 5186 (1981).
²⁶A. M. Semkow, P. Rosmus, H. Bock, and P. Botschwina, *Chem. Phys.* **40**, 377 (1979).
²⁷M. S. Gordon, D. R. Gano, J. S. Binkley, and M. J. Frisch, *J. Am. Chem. Soc.* **108**, 2191 (1986).
²⁸R. Walsh, *Acc. Chem. Res.* **14**, 246 (1981).
²⁹T. H. Dunning, Jr., *Chem. Phys. Lett.* **7**, 423 (1970).
³⁰Ze Jing and J. L. Whitten (unpublished).
³¹A. Hinchliffe, *J. Mol. Struct.* **48**, 279 (1978).
³²F. Stucki, J. A. Schaefer, J. R. Anderson, G. J. Plapeyre, and W. Gopel, *Solid State Commun.* **47**, 795 (1983).
³³H. S. Harold and D. Rapp, *J. Am. Chem. Soc.* **83**, 1 (1961).